Optics Communications 389 (2017) 212–223

Contents lists available at ScienceDirect

Optics Communications

journal homepage: www.elsevier.com/locate/optcom

Geometric plane shapes for computer-generated holographic engraving codes

Ángel G. Augier[a,*], Héctor Rabal[b], Raúl B. Sánchez[a]

[a] Instituto Superior de Tecnologías y Ciencias Aplicadas (InSTEC), Avenida Salvador Allende S/N, Quinta de Los Molinos, CP 10 600 La Habana, Cuba
[b] Centro de Investigaciones Ópticas (CONICET La Plata-CIC) and UID OPTIMO, Departamento de Ciencias Básicas, Facultad de Ingeniería, Universidad Nacional de la Plata, P.O. Box 3, 1897 Gonnet, La Plata, Argentina

ARTICLE INFO

Keywords:
Holography
Scratch holograms
Computer-generated holograms
Holographic engravings
Laser engraver systems
Information encoding

ABSTRACT

We report a new theoretical and experimental study on holograVures, as holographic computer-generated laser-engravings. A geometric theory of images based on the general principles of light ray behaviour is shown. The models used are also applicable for similar engravings obtained by any non-laser method, and the solutions allow for the analysis of particular situations, not only in the case of light reflection mode, but also in transmission mode geometry. This approach is a novel perspective allowing the three-dimensional (3D) design of engraved images for specific ends. We prove theoretically that plane curves of very general geometric shapes can be used to encode image information onto a two-dimensional (2D) engraving, showing notable influence on the behaviour of reconstructed images that appears as an exciting investigation topic, extending its applications. Several cases of code using particular curvilinear shapes are experimentally studied. The computer-generated objects are coded by using the chosen curve type, and engraved by a laser on a plane surface of suitable material. All images are recovered optically by adequate illumination. The pseudoscopic or orthoscopic character of these images is considered, and an appropriate interpretation is presented.

1. Introduction

Thin scratches on surfaces have interesting optical properties. In 1992, Plummer and Gardner [1] reported the discovery of holographic behaviour in lap abrasion, with three-dimensional effects; mechanically produced scratches acted as a reflection hologram.

Different approaches to a technique for obtaining images from regular scratches were reported in 1995 by Beaty [2], referring to some previous works mentioning the synthesis of 3D images [3–5]. Beaty developed the circular-scratch technique into a method for creating three-dimensional images. *Scratch holography* has been the usual name for describing these displays. In [6], Abramson affirms that for the first time, these 3D displays by scratch techniques were obtained by Weil, who introduced its patent in December 1934 in the UK [7], and referred to the technique as incoherent holography [8,9]. Others similar techniques in copper or aluminum metal are described in [10,11].

Some elements of the theory for such a “scratch” technique, and how scratches work in the formation of 3D images, have been discussed and explained from different particular viewpoints by Plummer and Gardner [1], Eichler et al. [12], and also by Beaty [13]. These theoretical analyses consider only the circular geometry of scratches. More recently, Brand [14] analysed geometrically, in a more general way, the shape of the surfaces for constructing specular holograms to be formed by fabrication techniques such as milling, grinding, stamping, ablation, etc. Duke [15] used hand-made and mechanical engraves of some particular curvilinear geometries to form abrasive holograms on aluminum plates and by an etching press.

HolograVures as computer-generated holographic laser-engravings using circular-arcs as code curves were presented by Augier and Sánchez [16–18]. This approach is a generalisation of the scratch-holographic record. Engravings and technology were created in order to allow the competitive use of these displays and to widen its applications, scope and quality by making computer-generated engravings directly by a laser. This technique allows reproduction of hologravures from an original computerised design. As in [16], we have conserved the general use of the term “holography” when referring to this technique of “scratches”, able to encode three-dimensional information, and to the corresponding reconstructed images. Although these displays are not holographic in the strict and original sense of that term, they possess a group of optical properties in common with conventional holograms [1,2,8,13]. Consequently, a

* Corresponding author.
E-mail address: aaugier@fisica.uh.cu (Á.G. Augier).

http://dx.doi.org/10.1016/j.optcom.2016.11.018
Received 8 July 2016; Received in revised form 8 November 2016; Accepted 11 November 2016
Available online 27 December 2016

holograve is also considered as a holographic-engraving process to record directly by laser an encoded "virtual-scene" from a 3D computer-generated world onto a 2D engraving, and to recover optically the original scene as a 3D reconstructed image from the real world, by means of appropriate illumination. Thus, for a determined size of the plate, undistorted stereo images can be observed for a wide range of viewpoints under an adequate position of the light source. Holograves have been exhibited in public art exhibits, in conditions of standard gallery illumination. An example in the transmitted light mode, showing photographs of appropriate quality, can be found in [19].

In these engravings, two-dimensional representations on the recording material are considered as a 2D code that allows the corresponding 3D object image to be recovered. When the engravings are recorded in transparent materials, the reconstructed images can be observed in both the transmitted and reflected illumination modes. Some interesting applications are shown in [16–18].

Considerations about the internal shape of scratches, as grooves, are not usually found in the thematic literature, although in isolated cases we can find some remark. For example, in [1] the circular scratches made by a lap on nickel plated aluminum piece was analised as curved line-scatterers reflecting the light equally in all radial directions, where each incoming ray is scattered as a hollow cone of rays. The line-scatterer is represented in [13] as a bent rod, and each ray from the point source produces conical sets of scattered rays. It is shown not rigorously how the images are formed; the circular line-scatterer produces both a reflection-mode image sent to one side of reference plane, and a transmission-mode image sent to the other. In [12] the intensity distribution of the fan beam produced by circular scratches is considered experimentally. This paper shows photographs from positions of a possible observer, of a single circular broad scratch with a semicircular profile produced by a turning lathe, illuminated by a light point-source in transmission mode. From each position, one can see two light spots at opposite sites on the scratch. In [16] the quality of the lines traced by the CO_2 laser on some materials, as acrylic, polycarbonate, acetate and glass was considered. Microphotographs of the scratches drawn by steel point or laser traces on these materials and measurements of scratch average width are shown. Except in the case of engravings on common glass sheets, where can be observed that the grooves are broken, the reconstructed images from holograves on other materials were qualitatively satisfactory.

The purpose of this work is to construct a basic theory of holograves founded on general principles of the light ray behaviour. This approach is a new theoretical and experimental study on general curvilinear-encoding of image information as a novel perspective, allowing the design of engraved images for specific ends. Curves of very general geometric shapes can be used for encoding 3D image information from virtual models onto a 2D engraving. The experimental study of particular cases of curvilinear codes, showing their influence on the 3D reconstructed images, is developed by means of the same CO_2 laser-engraver used in [16]. This technique allows an adequate comparison with theoretical analysis.

A sufficiently broad theory allowing the analysis of general curvilinear scratch-codes and its influence on the 3D images obtained from a holographic engraving has not been previously available in the thematic literature. This work contributes to a more complete background of this theory.

2. Holograves as computer-generated laser-engravings

According to Caulfield [20], the first computer-generated hologram known was made by Kozma and Kelly in 1965. Indeed, it was not used as a hologram, but as a complex spatial filter [21]. Pioneering work in this direction was also developed by Lohmann et al. [22].

Standard computer-generated holograms are usually of reduced dimensions and their use mostly restricted to work as diffractive optical elements in optical information processing. In other types of digital holography, information is typically recorded and recovered by a computer, with applications in areas like interferometry, microscopy, and data encryption [23]. Ordinary techniques for making computer-generated holograms [24] use a mathematical description of a virtual transparency. Typically, the calculated diffraction pattern first has to be plotted on an expanded scale and later photographically reduced. Other non-standard techniques, supporting computerised models and colour integral-holograms have been developed, including integral or stereographic holography, or similar technologies, and large format pieces, as for example in [25]. We will not mention here the numerous non-holographic computerised techniques to obtain 3D images that can be found in the Web.

Unlike the aforementioned techniques, a holograve [16–18] is an engraving and an image reconstruction process. In the first step, by using a laser-engraver, an encoded 3D computer-generated virtual scene is recorded on a suitable 2D medium, recovering later optically, in a second step, the original scene as a three-dimensional image. The light source is required to have very limited spatial extension. These processes are schematically shown in Fig. 1.

However, by using the same type of computer-generated code a similar holographic-engraving could be obtained by another process, able to record it on the medium, and obtaining the same 3D image by using the appropriate illumination. As the computer-generated scene is directly encoded, and reconstructed later optically, neither complex mathematical description, nor elements of standard computer-generated techniques are needed, and no characteristic technology of the integral stereographic holograms is used. The maximum size of these engravings is limited only by the dimensions of the work space of the laser engraver; therefore, it can generate pieces of large format. This technique also allows 3D images to be obtained by means of engravings, requiring very low resolution. The typical spatial frequency of the laser traces on the material is on the order of one or two lines per millimetre, although this number can be increased, depending on the application, the recording medium, and the characteristics of images and laser used to engrave.

Next we show, for circular scratch encoding, the basic correspondence between the points of the 3D model and the points of the holograve in the 2D plane. It was established in a very simple way in [16]. Note that these basic rules are contained in Fig. 1.

- Each point of the 3D model is coded as a segment of a circular curve in the hologram plane. The top of the curve matches the respective object point projection on that plane. (Observe 2D-encoded image from 3D model, to the left in Fig. 1a).
- For all the points of the 3D model that are at equal distance from the hologram plane, all the circular curve segments have the same radius.
- The distance between each point of the 3D model and the hologram plane is directly proportional to the radius of the corresponding coded circular curved segment. In this way, information about object depth is recorded.

Any available 3D virtual model computer generated could be represented in a 2D code by using some adequate encoding software and a CO_2 or other type of laser, as a tool for directly drawing the calculated scratch-codes on the suitable material. The power of the focused laser beam and its speed of movement on the material should be carefully adjusted.

Since the virtual depth of an image-point is proportional to the scratch radius, then the aperture angle of the circumference-arc is like the limit of a certain viewing angle, so that image only becomes visible at viewing angles.

Here, to appreciate the effects of depth, we show photographic stereoscopic pairs obtained from reconstructed 3D images. We use the illumination modes by either reflection or transmission. All images

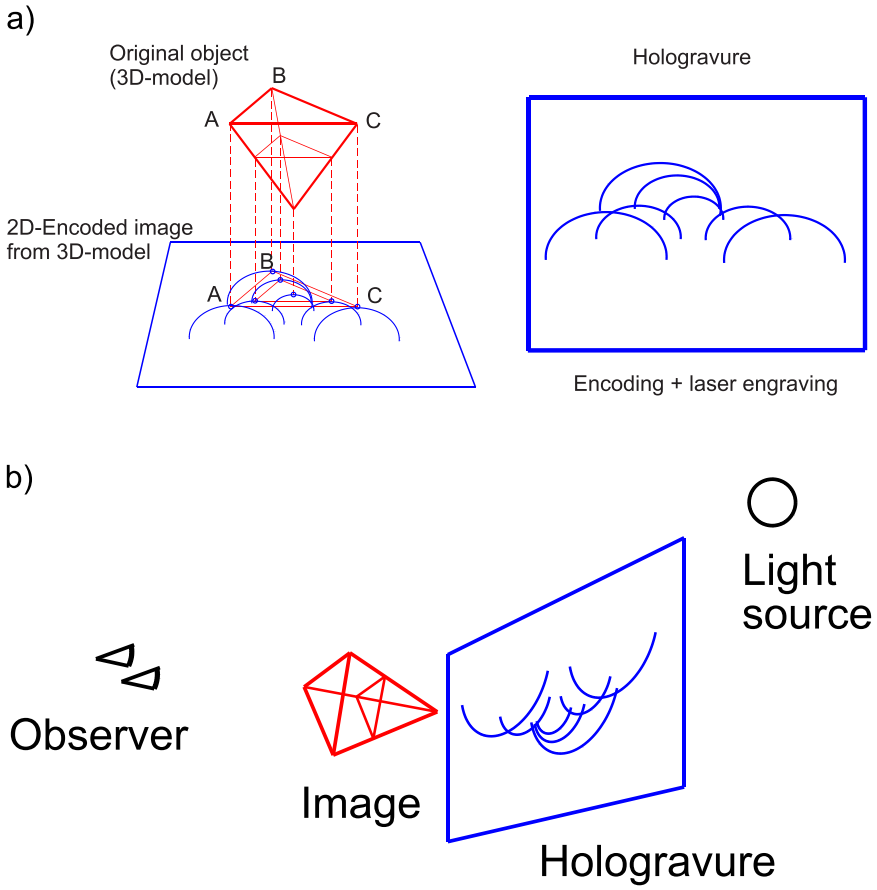

Fig. 1. Hologravure process using circular-arcs like curved codes, as is presented in [16]. (a) Step 1. Encoding and laser engraving process from a 3D-model, previously constructed by computer software. (b) Step 2. Image reconstruction from hologravure of recorded virtual original object.

were obtained using a 20 W halogen lamp.

In order to observe these photographic stereoscopic pairs, the reader should accommodate vision and convergence at an appropriate distance from the figure, or if necessary, use a simple stereoscope. The detailed observation of the three-dimensional images from the stereoscopic pairs is necessary for a clear understanding of the ideas expressed in this work.

2.1. Observing 3D images from engraved scratches

When a point from the virtual model has been encoded by a curvilinear laser-scratch on the suitable material, and a tiny straight segment of scratch is observed from a single point, as illuminated by a point like source, a bright, sometimes achromatic small region, due to scattering, reflection, and/or diffraction, can be observed. Other regions of the scratch are not seen as bright but for eventual stray light. Let us consider that a fine scratch curved segment, tangential to a unit vector T, is observable as a bright spot by an observer in O, under illumination from the light point-source in S, as shown in Fig. 2. Observe that points O and S could be either in the same side of the plane π, or on the opposite side of it, which keeps in mind the possibility of both modes: reflection and transmission of light. The bright spot can be observed from a particular point of view O, due to the light coming from each point P acting as a secondary light source.

If each point of a 3D virtual-object is coded with a different curve, for the observer's eyes and for a fixed light source position, a stereoscopic set of points forming a three-dimensional image of the original 3D model is obtained. The type of curve C belongs to a wide class of possible functions, defined on the plane, encoding the three-dimensional image information of model. Note that segment $O'S'$ is the projection on plane π of line OS. Both lines also belong to the plane Ω.

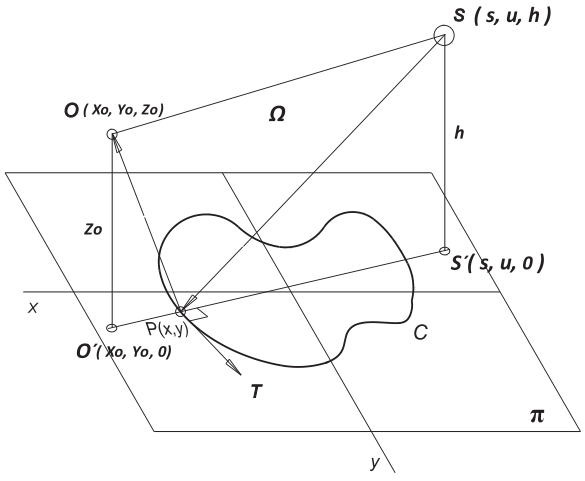

Fig. 2. Simple encoding with in-plane closed curved code. Light rays are represented as straight lines between the connecting points O, P and light-source S. The point P belongs to the curve C in the plane $\boldsymbol{\pi}$ of the engraving. A general study of this problem can be carried out by starting from the general principles of physics. In particular, Fermat's Principle in Optics [26,27] has been used in many cases for obtaining the laws of light behaviour.

Next we use Fermat's Principle to find the location of the bright spots on scratches of plane shapes used as codes, showing that the position of stereoscopic points can be predicted in a general way.

3. Fermat's principle and the observation of 3D images from holographic engravings

If an arbitrary type of curve is chosen to encode the points of the virtual object, each point of the 3D model can be coded with a segment of this curve in the hologram plane. In the step of image reconstruction, in adequate conditions for each position of the observer's eyes and for a fixed light source, a stereoscopic three-dimensional image of the original 3D model is obtained.

In the encoding step of the virtual object points, each closed curve used as code gives rise to two conjugated image-points. To avoid the duplication of reconstructed images, it is generally convenient to use an open segment of curve, allowing a single image to be obtained. Nevertheless, to carry out the theoretical studies of the image of stereoscopic points, it is appropriate to consider the complete closed curve to obtain the behaviour of the two conjugate points. In practice, different scales and lengths of the code-curve segments are taken.

Let us consider a geometric model to find the locus of the bright points P on the curves in the engraving plane, for each position of the observer's eyes O and for a fixed light source S.

Next, several geometric conditions are considered:

- The light source is given as a point-source.
- The observer's eyes are considered as observation points.
- The scratches are given as closed curves or curvilinear segments, without thickness.
- The engraving is considered a two-dimensional plate, like a defined region on the plane.
- Each observable bright curvilinear tiny-scratch-segment, tangential to a unit-vector T, is regarded as a bright point-spot.
- The three-dimensional reconstructed image is considered to be formed by a set of stereoscopic bright points.

According to Fermat's Principle, the optical path of a light ray moving with velocity $v(x, y, z)$ in an inhomogeneous medium between two points is an extremal of a functional, being necessary to find the extremal curves using the calculus of variations. A variational approach of this problem allows the most general and complex cases of non-plane scratch-curves and holographic surfaces to be solved. However, in our case, in a isotropic and homogeneous Cartesian space, it is well justified to affirm that the speed of light v is the same everywhere, and that light rays are straight lines along the paths between the connecting points. Under these circumstances, the problem reduces to the conditions of extremum (maximum, minimum or stationary estate) for the light ray path, taking as the investigated function the sum of Euclidean distances from the point-source S to observation point O, passing through a point P belonging to the curve C in the plane $\boldsymbol{\pi}$ of the engraving. The position and shape of the curvilinear scratch reduce the possible points P (x,y) of the plane to those satisfying the equation of the curved code $\Psi(x,y)=0$. To facilitate this mathematical work, we consider the engraving located on the plane $z=0$.

Let the arbitrary closed curve C be a scratch-code in a reference system of Cartesian coordinates, on the plane $z=0$. In this case, we have a problem of conditional extremum, which can be solved by using Lagrange's indeterminate multiplier method.

Given the curve $\Psi(x,y)=0$ as a constraint in the plane $z=0$, we need to find the necessary extremum condition of the sum of the Euclidean distances SP and PO, being $P(x,y)$ a generic point on this curve.

Let us consider the following affirmation:

> Light coming from a point-source at S, passing through the point P belonging to a curve C on the plane $\boldsymbol{\pi}$, will reach the observer's eye in O only when the sum of the Euclidean distances SP and OP between these points is a maximum, a minimum or, in general, a stationary value.

Light travelling along a straight line can be dispersed, reflected, refracted or diffracted at the point P. The mathematical function whose extremum we want to find is the sum of the Euclidean distances $L = L(x,y)$ and $D = D(x,y)$ between the considered points.

$$f(x, y) = L(x, y) + D(x, y) \tag{1}$$

where we define:

$$L = SP; \qquad L = \sqrt{(x - s)^2 + (y - u)^2 + h^2}$$
$$D = OP; \qquad D = \sqrt{(x_0 - x)^2 + (y_0 - y)^2 + z_0^2}$$

The coordinates of points S and O correspond to those shown in Fig. 1.

In order to find the solution with a conditioned extremum, we build the auxiliary function

$$F(x, y) = f(x, y) + \lambda\, \Psi(x, y) \tag{2}$$

where from (1) $f(x,y)$ is the sum of L and D, the constraint equation is $\Psi(x,y)=0$, and λ is a Lagrange's undetermined multiplier.

3.1. System of equations for finding the image point

Considering the necessary extremum condition, the solution can be obtained from the following general system of equations:

$$\begin{aligned} &\tfrac{\partial f}{\partial x} + \lambda \tfrac{\partial \Psi}{\partial x} = 0 \\ &\tfrac{\partial f}{\partial y} + \lambda \tfrac{\partial \Psi}{\partial y} = 0 \\ &\Psi(x, y) = 0 \end{aligned} \tag{3}$$

In order to solve the system (3), eliminating λ from the first two equations, we define a family of vectors $\boldsymbol{U}=\boldsymbol{U}(x, y)$ that in matrix form can be written as:

$$\boldsymbol{U} = \begin{bmatrix} \frac{x - s}{L} + \frac{x_0 - x}{D} \\ \frac{y - u}{L} + \frac{y_0 - y}{D} \end{bmatrix} \tag{4}$$

Taking into consideration that the direction of gradient $\nabla\Psi$ is the direction of vector N, normal to curve $\Psi(x, y) = 0$, if T is the tangent vector to this curve, then for all the points P perceived by the observer's eye in O, system (3) can be written in equivalent vector form as:

$$\begin{aligned} &\boldsymbol{T} \bullet \boldsymbol{U} = 0 \\ &\Psi(x, y) = 0 \end{aligned} \tag{5}$$

where the first equation in (5) is the scalar product of the two vectors.

If the vectors $\boldsymbol{T}= \boldsymbol{T}(x, y)$ and $\boldsymbol{U} = \boldsymbol{U}(x, y)$ are written in matrix form

$$\boldsymbol{T} = \begin{bmatrix} \frac{1}{\sqrt{1 + \left(\frac{dy}{dx}\right)^2}} \\ \frac{\left(\frac{dy}{dx}\right)}{\sqrt{1 + \left(\frac{dy}{dx}\right)^2}} \end{bmatrix} \qquad \boldsymbol{U} = \begin{bmatrix} U_x \\ U_y \end{bmatrix} \tag{6}$$

then the previous system of Eq. (5) can be written as

$$\begin{aligned} &U_x + U_y \tfrac{dy}{dx} = 0 \\ &\Psi(x, y) = 0 \end{aligned} \tag{7}$$

where U_x, U_y are the components of vector $\boldsymbol{U}$ in the x and y directions respectively, and the derivative is

$$\frac{dy}{dx} = \frac{-\frac{\partial}{\partial x}\psi(x, y)}{\frac{\partial}{\partial y}\psi(x, y)}$$

Notice that, for single-eye observation, a bright spot P is located at the point of the scratch where the tangent to the curve is perpendicular to vector $\boldsymbol{U}$.

Each eye can see separately a different bright point on the open scratch. Thus, as each eye observes the engraving plane under different

parallax, the two required points of view for forming the stereoscopic image are obtained.

The relations (5) and (7) indicate that for each point $P(x,y)$, the solution of the system (3), the tangent vector T to the curve C is perpendicular to each vector $\boldsymbol{U}=\boldsymbol{U}(x,y)$ of a family satisfying (5). It can be proven that a common spatial direction exists for the vectors $\boldsymbol{U}$, and that they are in the direction $O´S´$ for any curve C.

Thus, the previous statement can be expressed for any curve $\Psi(x, y) =0$, and for any real number β, as:

$$\boldsymbol{U}\ (x,\ y)\ \ =\ \beta\ \ \boldsymbol{U}_0$$

We will take a vector of this family; the constant vector $\boldsymbol{U}_O$ defined in the form

$$\boldsymbol{U}_0 = \begin{bmatrix} x_0 - s \\ y_0 - u \end{bmatrix}$$

Thus the system (3) becomes:

$$\begin{aligned} &\boldsymbol{T} \bullet \boldsymbol{U}_0 = 0 \\ &\Psi\,(x,\ y) = 0 \end{aligned} \tag{8}$$

where the vector $\boldsymbol{U}_0$ is contained in the plane $\boldsymbol{\Omega}$.

Although system (8) is expressed in Cartesian coordinates, by having the scalar product of vectors, the fundamental property of being independent of the system of coordinates specific to which the space is referred, the Eq. (8) have general validity and constitute the expression of a geometric condition. For the relative positions of the point-source and observer, at S and O respectively, the bright spot P is located at the point of the scratch where the tangent vector $\boldsymbol{T}$ to the curve Ψ is perpendicular to vector $\boldsymbol{U}_O$. The solution is determined by the geometric model's conditions defined above.

Notice that, according the theoretical results obtained by using the Fermat Principle the point P on any arbitrary curved code is situated at the point where the vector T, tangent to the curve, is also perpendicular to the plane SPO, called Ω in Fig. 2. The mathematical form of this statement is expressed by the equations system in form (8).

In the solution of system (3), no approximation has been made. Observe that, as a consequence of the geometric relationships among the source, the observer's position and the bright spots on curve C, system (8) is useful, not only in the case of light-reflection mode, but also for light-transmission mode geometry.

It can be verified directly that for our reference frame, the previous system of equations can be written in the following simple general form:

$$\begin{aligned} &(x_0 - s) + \ (y_0 - u)\frac{dy}{dx} = 0 \\ &\Psi\,(x,\ y) = 0 \end{aligned} \tag{9}$$

Note that:

- All points $P(x,y)$ obtained as solutions lie on the curve $\Psi(x,\ y) = 0$
- All observers situated in the line OS will see the same bright points P on the closed curve C.
- The Euclidean 3D distance from the source S to the observer O is a constant, and also the projection $O´S´$ of this line on plane π. To find the bright points on the curve C, we need the projections $O´S´$ on the plane π of the engraving.
- The code-curve C can be a simple closed curve of arbitrary shape, being relevant for obtaining special behaviours of the reconstructed images.

Bearing in mind the aforementioned remarks, we can see that there are several ways to change the location of the bright point for an observer: by changing the source and/or observer position, by changing the shape of the curve C with the corresponding local orientation of the vector $\boldsymbol{T}$, and by tilting the plate in different ways.

4. Study and comparison of some simple cases

The use of non-circular codes in the engraving can modify the stability and spatial position of the observed images. This analysis is useful for all "scratch" holographic engravings. Both the circumference and ellipse are some of the conic sections. A case of particular interest is the elliptic code. Parabola and hyperbola, as plane codes of conic sections are not studied here.

4.1. Elliptical arcs as segments of conic sections

When the curve C is a canonical ellipse, to find the bright points we need solve system (9) with the constraint:

$$\Psi(x,\ y) = \frac{x^2}{b^2} + \frac{y^2}{a^2} - 1 \tag{10}$$

where a and b are the semi axes of the ellipse.

The solutions are two bright points for each position of the source S and the observer's eye O. The direction $O´S´$ on plane π is the same as that considered before.

We obtain:

$$x_1 = \pm\frac{b^2}{\left(a^2\left(\frac{y_0-u}{x_0-s}\right)^2 + b^2\right)^{1/2}} \qquad y_1 = \pm\frac{a^2\left(\frac{y_0-u}{x_0-s}\right)}{\left(a^2\left(\frac{y_0-u}{x_0-s}\right)^2 + b^2\right)^{1/2}} \tag{11}$$

In Fig. 3 are represented the projections on the plane of the observer's eye at coordinates O_1' and O_2' and of the light point-source at coordinate $S´$. Each eye can see separately two bright points P on the ellipse. The observer's eyes can only see the represented spots on the curve. In Figs. 3 and 5 we will suppose that the units of length are given in cm.

Notice that in Fig. 3, the bright spots observed by each eye lie on two different lines belonging to the plane of engraving. For the eye at O_1 they are represented as dotted lines parallel to direction $O_1'S'$. Thus, the observer's eye at $O_1(2, -8, h)$ can see only the points on these dotted lines. For the eye at $O_2(9, -8, h)$, the two corresponding parallel lines to direction $O_2'S'$ are not represented.

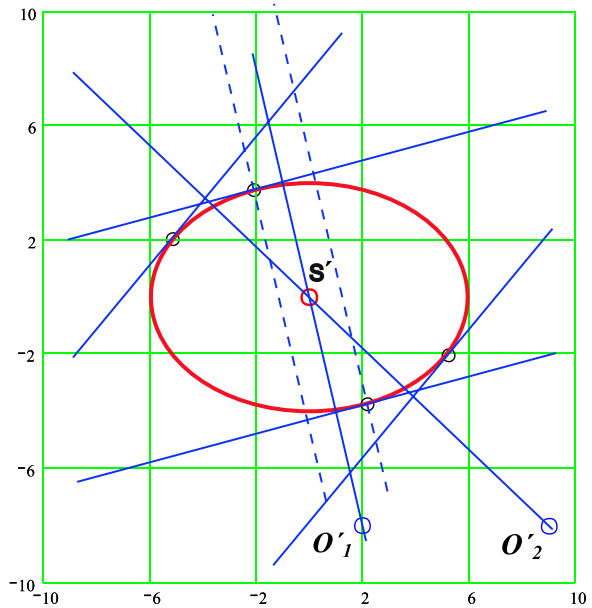

Fig. 3. Elliptic code in the case of a =4, b =6, and source S located at height h, with coordinates on the plane π at s=0, *and* u =0, and the bright spots observed from points O_1 and O_2, with in-plane projections $O´_1$ and $O´_2$. For this ellipse is b/a =1.5.

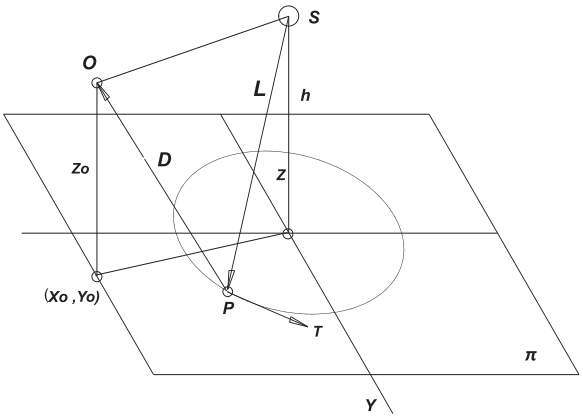

Fig. 4. Particular geometry with a circle as the curvilinear "scratch-code" and the light source located at height h from the centre, coinciding with the origin of coordinates.

4.2. Circular code as a particular case

In [1], Plummer and Gardner analysed a simple case, in reflection mode, for a circular scratch. This is a particular geometric study, approaching the solution to the case of a far source and vertical illumination.

Next, we consider the circular geometry, comparing our results using system (9) to those obtained in [1].

If curve C is a circumference of radius R, then to solve the system of Eq. (9), for every position of the source S and the observer's eye O, we have the constraint

$$\Psi(x, y) = x^2 + y^2 - R^2 \tag{12}$$

The slope of a straight line in direction $O´S´$ of plane π is $m = \frac{y_0 - u}{x_0 - s}$. The straight line, perpendicular to this direction, being tangential to the scratch curve can be obtained; the solutions are two bright points, (x_1, y_1) and (x_2, y_2), for each position of the source S and the observer's eye O. Fig. 4 shows the source S over the centre of the circumference, coinciding with the origin of coordinates, at height h.

The projection of the point-source S on the plane is at the origin of coordinates. We can solve Eq. (9) with constraint (12), for $s=0$, $u=0$. In this case, we obtain the same result more easily by taking a = R, $b = R$ in (11).

$$x_1 = \pm \frac{R}{\left(\left(\frac{y_0}{x_0}\right)^2 + 1\right)^{1/2}} \quad y_1 = \pm \frac{y_0 \; R}{x_0\left(\left(\frac{y_0}{x_0}\right)^2 + 1\right)^{1/2}} \tag{13}$$

The bright points perceived by the observer's eyes at O_1 and O_2 are shown in Fig. 5. The straight lines in directions containing the projections $O_1´S´$ and $O_2´S´$ on the plane π pass through the origin. The straight lines perpendicular to these directions are also represented.

From the above example, for a circumference of radius $R=4$, and the points at $O_1´(-3.5, 8)$ and $O_2´(3.5, 8)$, the eye at O_1 can see the points $(-1.603, 3.665)$; $(1.603, -3.665)$, on the line $O_1´S´$ while the eye at O_2, can see the points $(1.603, 3.665)$; $(-1.603, -3.665)$, on the line $O_2´S´$.

5. Stereoscopic effect

We are able to perceive depth in 3D space because we have two eyes separated horizontally by a certain distance. The stereoscopic vision is possible when each eye of a binocular observer watches the same scene from a slightly different perspective.

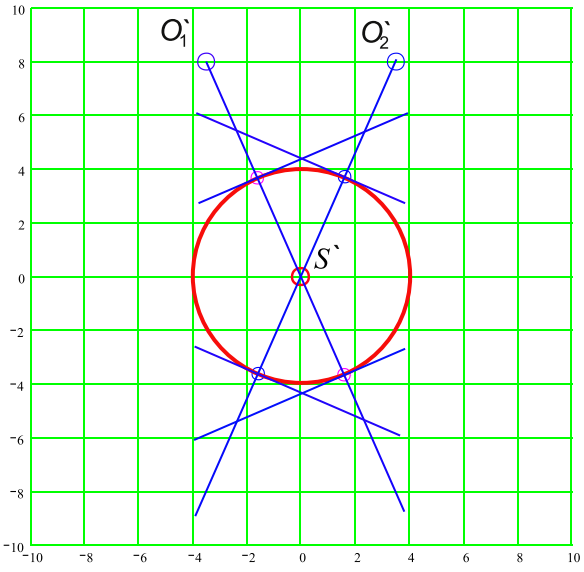

Fig. 5. The projections of the observer's eyes on the plane π are at the points $O_1´$ and $O_2´$, in such a way that at a particular instant each eye can see, separately, only two bright points P on the circumference.

5.1. Coordinates of stereoscopic points

If each eye of the binocular observer sees the bright spot on the curved scratch at a different place, and if both positions of the bright points are observed adequately displaced in the direction of the eyes' separation, a single stereoscopic point is perceived as floating in front or behind of the scratched plate, depending on the sign of the curvature. The observation of the stereoscopic effect by a binocular observer is also called stereopsis.

The position of stereoscopic points in the case of circular scratches and frontal illumination was considered in [1,12].

A more general study shows that there are two possible models to explain stereoscopic images from holographic engravings. These models would be appropriate, depending on interior profile of scratches and physical phenomena that give rise to images. Each model gives the two possible image configurations; in front and behind the reference plane.

The observation of the stereoscopic points for bright spots on an ideal circular scratch is shown in Fig. 6a, according to model described in [1].

The observation of the stereoscopic effect according to the alternative model presented in this work is shown in Fig. 6b, where we can see the stereoscopic images in front or behind the engraving plane, but they have been inverted or changed in their relative position with respect to the engraving plane.

In a general case, by using the solutions to system (9), and considering the rectilinear propagation of the light, we can obtain the coordinates of the stereoscopic points by solving a system of two linear equations in three dimensions for each pair of points (x_1,y_1), (x_2,y_2) having parallax. In vector form, the two straight lines from each observer's eye to the bright spots at curve C, as a linear system of parametric equations, is given as:

$$\mathbf{r} = \mathbf{r}_{01} + \mathbf{S}_1 t$$
$$\mathbf{r} = \mathbf{r}_{02} + \mathbf{S}_2 t \tag{14}$$

where t is a parameter; $1 \geq t \geq 0$.

By representing the vectors in matrix form we have

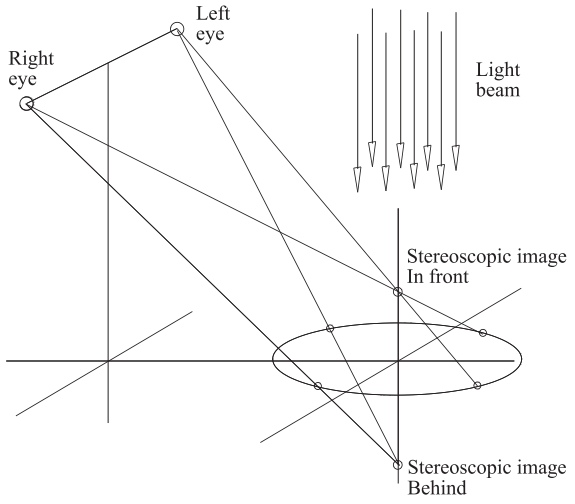

Fig. 6. Stereoscopic points perceived by a binocular observer in the circular-scratch geometry. a) As is considered in [1]. Stereoscopic points at *x=0*; *y=0*; and z-coordinates in front and behind of the engraving plane. b) According to alternative model considered in this paper. Stereoscopic points at x=0; y≠0; z-coordinates also in front and behind the plane.

$$\mathbf{r} = \begin{bmatrix} x \\ y \\ z \end{bmatrix} \quad \mathbf{r}_{01} = \begin{bmatrix} x_0 \\ y_0 \\ z_0 \end{bmatrix} \quad \mathbf{r}_{02} = \begin{bmatrix} -x_0 \\ y_0 \\ z_0 \end{bmatrix}$$

$$\mathbf{S}_1 = \begin{bmatrix} x_1 - x_0 \\ y_1 - y_0 \\ -z_0 \end{bmatrix} \quad \mathbf{S}_2 = \begin{bmatrix} x_2 + x_0 \\ y_2 - y_0 \\ -z_0 \end{bmatrix}$$

where we suppose that the reference plane is z=0 and that symmetry exists in the "x" axis respect the origin for the observer's eyes.

In this way the solution for the stereoscopic image point *(x, y, z)* in front of the engraving is

$$x = -x_0 \frac{(x_1 + x_2)}{(x_2 - 2x_0 - x_1)} \quad y = \frac{(y_0 x_2 - y_0 x_1 - 2x_0 y_1)}{(x_2 - 2x_0 - x_1)} \quad z = z_0 \frac{(-x_1 + x_2)}{(x_2 - 2x_0 - x_1)} \tag{15}$$

And the stereoscopic image point *(x, y, z)* behind the engraving is

$$x = x_0 \frac{(x_1 + x_2)}{(x_2 + 2x_0 - x_1)} \quad y = \frac{(y_0 x_2 - y_0 x_1 + 2x_0 y_2)}{(x_2 + 2x_0 - x_1)} \quad z = z_0 \frac{(-x_1 + x_2)}{(x_2 + 2x_0 - x_1)} \tag{16}$$

where $2\times_0$ corresponds to the inter-pupillary distance.

Note that for the particular symmetrical circular conditions and from the position of the observer's eyes and the light source, the coordinates of bright spots on the circle satisfy x_1=-x_2; y_1= y_2; *and* y_0/x_0= y_1/x_1.

In this particular case, we have two possible solutions.

First, for *x=0; y=0,* we can find and writing for the points of the stereoscopic images the *z*-coordinate solutions:

$$z_\pm = \pm z_0 \frac{x_2}{(x_0 \pm x_2)}$$

From aforementioned symmetrical circular conditions, these solutions can be written in this case as:

$$x = 0 \quad y = 0 \quad z_\pm = \pm z_0 \frac{R}{\sqrt{x_0^2 + y_0^2} \pm R} \tag{17}$$

In Eq. (17), the sign (+) corresponds to the image in front of the engraving and the sign (-) to that behind the engraving. This result is in good agreement with the solutions obtained in [1] from geometrical considerations for this particular case.

From the same system of Eq. (14) we have the possibility to obtain a different images configuration.

The second solution we can find for $x=0; y \neq 0$

$$x = 0 \quad y_\pm = \pm y_0 \frac{2R}{\sqrt{x_0^2 + y_0^2} \pm R} \quad z_\pm = \pm z_0 \frac{R}{\sqrt{x_0^2 + y_0^2} \pm R} \tag{18}$$

Observe the representation of stereoscopic effect according this model in Fig. 6b.

Notice that in both models, for the same conditions of illumination and observation, and equal radius of scratch, the stereoscopic image-points appear at the same z-coordinates.

5.2. A graphical geometric approach from the solution of system of equations

As a consequence of the general validity and geometric sense of (8), we can approach to solutions of system of Eq. (9) in graphic form, finding the locus of the bright spots. In the same way, by taking like data the solutions from (9), the locus of stereoscopic points can be obtained considering the rectilinear propagation of the light.

Such a graphic representation would be adequate, in certain cases, to describe the geometry of a complex system of specific encoding curves or when a rigorous solution is not necessary. It would be also convenient as a reference, before or after solving the corresponding system of equations.

Next we describe a set of geometric steps, valid for arbitrary shape plane codes. The stereoscopic point can be found by means of step 4 after finding the position of the bright spots on a code-curve by steps 1–3.

1. Find the straight line segments from the point-source *S* to the observation point *O*, for each observer's eye.
2. Find the projections on the plane π of the straight line segments obtained above. These lines will be considered as a reference.
3. Determine the perpendicular to each segment of straight line *O´S´* projected on the plane, so that they are also tangents to curve *C*. The points of tangency on *C* are the coordinates of the bright spots observed from each point *O*.
4. Find the straight lines from the points *O* of each eye to the spots found in step 3 on the plane, and draw these lines connecting the considered points in the 3D space. Determine the stereoscopic points at the intersection of the straight lines. In the case of model described in [1], if the bright spots on curve *C* are observed from the concave curvature side, the lines cross before the spots and the stereoscopic point is "in front". If the bright spots on curve *C* are observed from the convex curvature side, the lines cross behind the spots and stereoscopic point is "behind". In the case of the alternative model presented here, this rule is inverted.

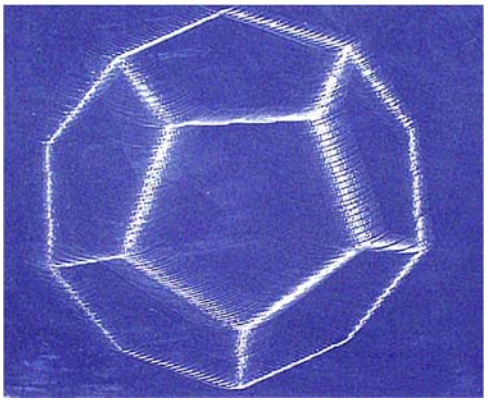

Fig. 7. Photograph from 3D image of a polyhedron engraved on acrylic plate, obtained in reflexion mode. The plate was rotated 180° in-plane for obtaining the adequate conditions of illumination and observation from the concave or convex curvatures of the codes mentioned in Table 1.

Observe the two cases of the stereoscopic effect shown in Fig. 6a and b.

5.3. Experimental study of stereoscopic image

For the experimental study of image characteristics, we used the 3D image of a polyhedron obtained from hologravure shown in [19]. This polyhedron is engraved on a transparent 27.94×35.56 cm acrylic sheet. This study is useful to understand how the 3D images are perceived by the observer in front or behind of the scratched plate.

A polyhedron is a relatively simple geometric figure that allows its three-dimensional form and possible deformations to be easily appreciated. A photograph from the corresponding 3D image, in front of the engraving, is shown in Fig. 7, where the geometry for reconstructing the image is similar to that shown in Fig. 4, but the used code-shapes are segments of circumferences of variable radius, opening upward.

The results show that both the conditions of illumination and observation are relevant with respect to the relative position of the curve-code curvature. According to these conditions, the 3D image can be observed in front or behind the engraving plane. The results are summarised in Table 1, where we considered concave (curving inwards), and convex (curved outwards), regarding the relative position of the circular-segments to the source of light, or to the observer.

5.4. Observation of orthoscopic or pseudoscopic images

Three-dimensional images optically reconstructed from holograVures can be observed as orthoscopic or pseudoscopic images.

An image is orthoscopic or pseudoscopic, “correct” or "incorrect", with respect to a certain reference object. In the case of these computer-generated engravings, this reference is the image that the user of the computer software builds in the 3D image editor. This original image, located in a reference screen, is our “object”, which is, in the “computerised” sense of the term, virtual. To this image it is necessary to refer to any correctness or incorrectness.

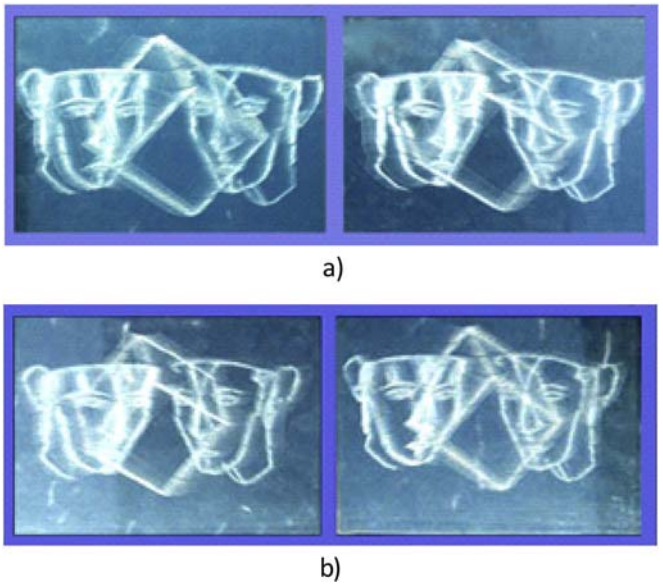

Fig. 8. Photographic stereoscopic pairs from a 3D complex scene, laser engraved on thermo-resistant acetate piece. Reconstructed 3D image was obtained in reflection mode. a) Orthoscopic image. b) Pseudoscopic image.

Usually, when we consider open curves as scratches, and the engraving is illuminated in reflection mode, from the concave side of the engraved curves, a 3D image will be observed in front of the engraving plane. If, under the same conditions, the engraving is illuminated from the convex side of the curves, the observed image will be behind the plane. A similar analysis can be made when images in the transmission mode are obtained.

Thus, when the reconstructed image from the holograVure is like our “virtual-object”, it is correct, and we call it orthoscopic. In the case of depth inversion, the optically reconstructed image is incorrect (i.e. depth reversed), and we call it pseudoscopic. The 3D image from the polyhedron, in front of the plate, which is shown in Fig. 7 is an orthoscopic image, because it is like the original virtual object: a computer-designed convex polyhedron. We obtain a more complex case if the image contains several objects. Fig. 8 shows two stereoscopic photographic pairs obtained from the 3D reconstructed images of a complex scene. Note that when the light source is above the level of the engraving plate (Fig. 8a), we observe in front of the plate, for the corresponding stereoscopic image: first, the cube; secondly, the face on the right; and finally the face on the left. As a result of the previously obtained computer-generated virtual model, the author of the designed scene has defined this display as the orthoscopic image.

If for the same engraving the light source is below (Fig. 8b), the reconstructed scene appears to be inverted with respect to the distances from the plane of the engraving to the viewer, being then observed behind the plate. The author of the designed scene has defined this inverted display as the pseudoscopic image.

A similar effect happens to images of objects from the real world obtained in conventional holography, by using as a reconstruction

Table 1
Experimental study of the stereoscopic image position from holograVure with respect to the curve-code curvature for reflection mode, according to the conditions of observation and illumination.

Case	Curvature illumination		Curvature observation		3D-image position	
	concave	convex	concave	convex	behind	Infront
1	x			x		x
2		x	x		x	
3		x		x	x	
4	x		x			x

beam the reference beam or its conjugate.

6. Study of some curved-code shapes

We have seen how the geometric theory obtained from the fundamental laws of light rays behaviour leads to formation of holographic-engravings images. We concern with a very general shape of scratches, different scales, and resolution. Such a general theory does not concern a specific physical process, but only the ability of the possible processes so that the light arrives from the spots to the observer.

When a curved scratch is observed with both eyes, different light spots are seen on it with the right and the left eye, so that each eye sees separately images from a slightly different perspective, independently of the physical process used to obtain them. Stereopsis leads observers perceiving both images to observe the combined stereoscopic spot appears in front or behind of engravings plane.

6.1. Interior profile of the grooves

In the space allowed for this paper, we have only been able to introduce the geometric theory for plane-shape coding scratches, obtaining the tree-dimensional images and discussing the conceptual models. The problem considering the internal shape of scratches as grooves is far too from our objectives to allow a complete analysis here. We may, however, consider a few remarks concerning some of the simpler aspects of this problem.

We can see that according to the specific physical process and the observation mode required for a type of image, a certain technological process and an engraving material will be more appropriate to record image information, and the grooves would have a different interior geometry. So, the interior shape of the grooves could have a different profile for different technological processes. This profile and the involved physical phenomenon and technology determine the image quality and contribute to its behaviour.

The quality of the lines traced on some materials, as acrylic, polycarbonate, thermo-resistant acetate sheets and glass were studied by us in [16], where there are presented measurements of average width of scratches for several representative engravings, as well as microphotographs of engraved grooves.

When one draws directly with steel needle on an appropriate material a hand-made hologram,

-simpler version of the scratch technique- the produced drawn grooves conserve in their interior profile a similar form to the road left by the tip of the needle moving on the material. In this case we haven't a previous computerised drawing. The final result obtained by the tip of the needle in a continuous curved form and the grooves take a continuous profile depending only of the hand movement of the draftsman. In our present paper, stereoscopic images from Fig. 9a, b and Fig. 11b were coded hand-drawn, directly with steel point on acetate sheet.

In the case of holograVures, they are computer-generated and laser engraved scratch holograms, made by a cw CO2 laser focused beam [19]. In [16] it is described how the engraver-laser system uses a lens forming a focal spot of a few micrometers in diameter. It is well known that in these cases the profile of power in the focused region could approaches to Airy-Disk of the Function of Airy, due the diffraction process of the light in the focusing lens. In consequence, the cw laser heats and softens the material. The intensity of the focused laser beam and his speed of movement on material are carefully adjusted for just slightly vaporizing the surface of the material, leaving a groove on it.

The experimental evidence in [16] suggests that in the cases considered, due to the nature of the processes used to record, scratched grooves of usual holographic engravings made on adequate materials could have internal profile approaching to the road left by the engraving tool on the material; the top of the needle or steel point, or the focused laser region.

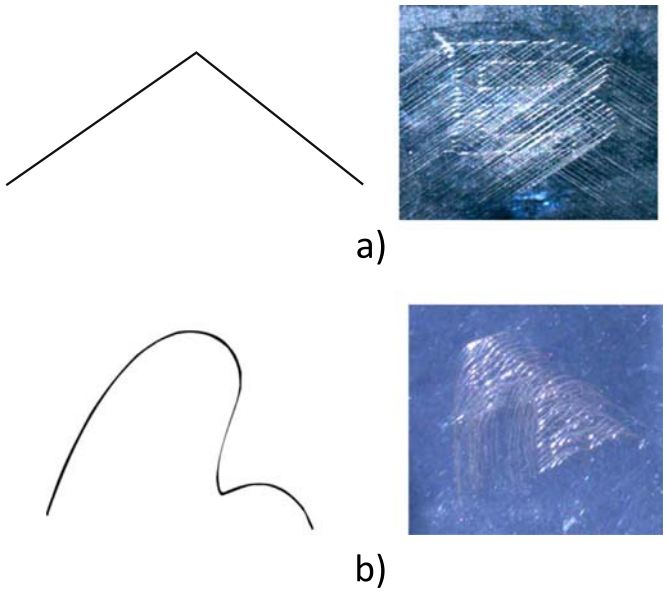

Fig. 9. Photographic images obtained by using simple geometrical shape codes. a) Letter *B*, obtained by using a triangular form code. b) Letter *A* is encoded by an "undulated" code.

It is an experimental fact that engravings made by certain mechanical processes [1,10,11] or by a needle or steel point [13,16]; or the holograVures, made by a focused laser beam [16–19]; or engravings made by others fabrication techniques [14,15], they produce 3D images of appreciable good visual quality.

Nevertheless, it is appropriate to stand out that the question of the efficiency of the grooves profile, as well as the related problem of how obtaining an optimal quality of holographic engraving images by scratch techniques, it is an open and not yet solved problem constituting itself a topic for a new research. In all the cases, it will be necessary to verify rigorously any hypothesis or result experimentally determined, however, what is firm evidence is that the holographic engravings, as they are described in our paper, are able to obtain good images, and that our model is able to describe rigorously its behaviour.

An optimal image quality is a concept depending on the type of image considered and observation mode, and deserves a special study including the internal profile of the grooves, the relief and characteristics of the engraving material and recorded surface, and the detailed analyses of involved technological processes, and its consequences.

It is remarkable that our geometric approach in this work doesn't consider any of these questions in explicit form; however, based on the Fermat Principle and the behaviour of the rays of light we have demonstrated that it can describe rigorously the position of the light spots on scratches perceived by observers, the locus of the stereoscopic image-points and the behaviour of these 3D images regarding their relative position, behind or in front the reference plane. The commented facts show that the results obtaining from any physical process and technology allowing to the light rays to satisfy the Fermat Principle could be described.

In the case of circular codes (see Fig. 6a and b), a simple example shows an adequate model to describe these images, by using as solutions either expression (17) or (18); for the case of pitch lap (polishing disk) engraving image-process on a nickel plated aluminum flat, described in [1], or for the case of hand-drawn scratch holograms made by steel tip on acrylic [13,16], or for engravings made by a focused laser on some plastic materials [19].

6.2. Experimental study of some plane curvilinear codes

We have seen that a simple type of plane curve can be used to code

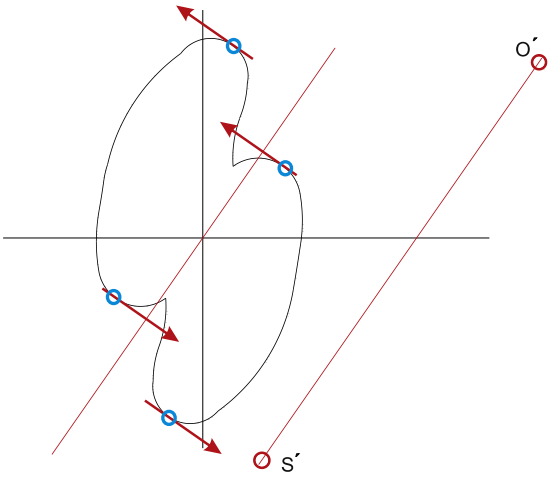

Fig. 10. Closed "undulated" code, where the bright points have been found theoretically. The points S´ and O´ are respectively the projections of point-source and observation point on the plane. The tangent vectors to the curve, and perpendicular to the direction S´O´, are represented.

the image of a computer-generated “virtual” object on the engraving plane. Fig. 9 shows the use of simple geometrical forms for encoding the image information. The open curves as scratches are drawn on.

We show encoded letter images by using two simple geometrical shapes. The letter *B* was obtained by a triangular code, and an “undulated” code was used to codify the image of the letter *A*. For the undulated code, we observe two reconstructed images of the original letter. The appearances of the position and depth of these images of letters depend on the relative size and inclination of each lump-wave form; the image is repeated according to the number of crests in the undulation. Consequently, each lump from the encoded curve-shape acts as a separated single curve, giving a resulting image.

A closed “undulated” code is represented in Fig. 10, where the bright image spots on curve *C* have been found theoretically from the set of practical geometrical steps shown above. The corresponding open code allows two images to be obtained, according to the number of “crests” in the undulation, as shown in Fig. 9b.

6.3. Codification by elliptical arcs

The size of the curve used as code determines the visual effect of depth in the 3D image points; however, if the curve is an ellipse, their eccentricity determines other effects. In order to describe the form of the curve for elliptical codification, we need a geometric parameter. Although the usual parameter for describing an ellipse is its eccentricity ε, which is in the interval,$1 \geq \varepsilon \geq 0$, for us a more useful parameter can be defined as the ratio $r = b/a; r \geq 0$.

The elliptical geometry described by the relative parameter r is shown in Fig. 11a. In a more general case, the ellipse could be inclined in a plane with respect to the rectangular Cartesian axes. In this case, if *"x"* is the abscissa axis, we also take as a parameter the angle α with respect to this horizontal axis. Fig. 11b shows a photographic stereo pair from a 3D image of the letters *A, B,* and *C* coded by a steel point on an acetate sheet. Observing the 3D image, we can see that the letters appear in planes of different depth, in front of the scratched plate. A small rotation of the letter *C* is observed, which changes between the two angular positions of the pair, when the observation point moves in a horizontal direction. The letters *A* and *B* show a better stability. They were encoded using ellipses of different sizes but identical parameter r =0.595. The letter *C* was obtained by circular encoding (r =*1*).

Fig. 12a and b show photographic stereoscopic pairs from images of two letters *A* obtained by using computer-generated elliptical segments as codes. The reconstructed 3D images are observed behind the scratched plate, in transmission mode. For these plane letters, the

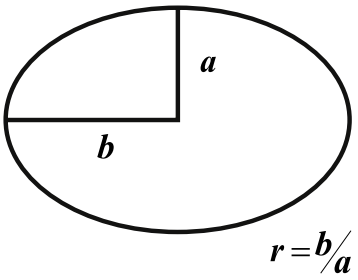

a)

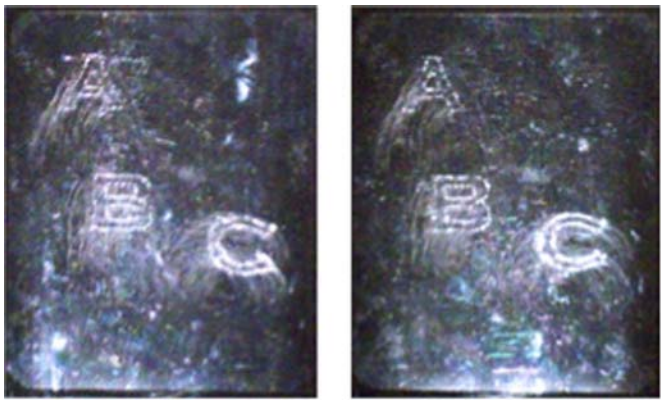

b)

Fig. 11. Codification by elliptical arcs; a) Elliptic geometry described by the relative parameter *r*. b) Stereoscopic pair from scratch-holographic image of the letters *A, B*, and *C* engraved directly hand-drawn by a steel point on acetate sheet. Reconstructed image was obtained in reflection mode.

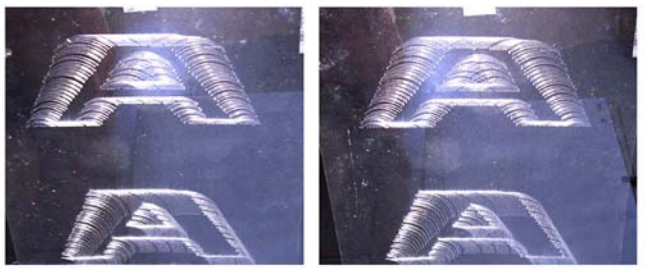

a)

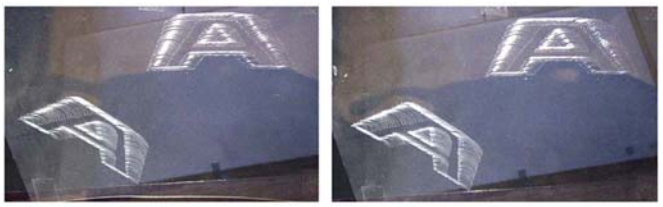

b)

Fig. 12. Stereoscopic pairs containing two flat letters *A*. a) both encoded letters are vertical, but the elliptic codes of the letter appearing below are inclined at the angle α=45° with respect to horizontal axis *“x”*, b) both encoded letters are at different angle, but the elliptic codes of the letter appearing below are inclined at the angle $\alpha=45^0$ with respect to letter axis. In all the cases stereoscopic images of the letters appear in planes with different spatial orientation.

codes were designed by means of a version of the graphic design software CorelDraw. Holograves were laser-engraved on thermo-resistant acetate pieces. Note the different effects of “stand up” of 3D images from stereopairs and spatial inclination of the letters. The spatial inclination of the 3D-plane of the flat letters is produced by the

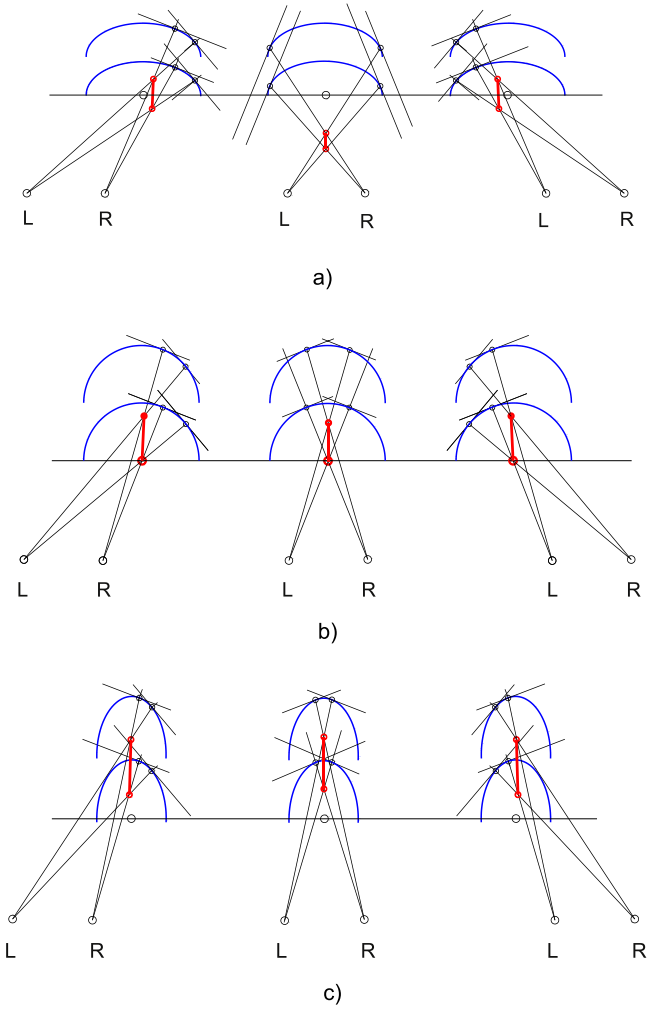

Fig. 13. Scheme for three positions of a pair of vertical encoding curves showing the observer's eyes moving horizontally on abscissa axis; a) elliptic curved codes with $r > 1$, b) circular curved codes with $r = 1$, c) elliptic curved codes with $r < 1$.

inclination of elliptic axes. In Fig. 12a, the upper letter is upright but the lower is inclined by $\alpha = 45°$ with respect to the vertical axis of the elliptical code. In Fig. 12b, the long axes of the elliptic codes coincide with the symmetry axes of each letter.

The application of symmetric or asymmetric codes provides interesting 3D effects, because in a simple way it is possible to change the inclination of a flat stereoscopic image regarding the engraving plane. Symmetric elliptic code changes this inclination in uniform way, but asymmetric codes "twist" the plane.

6.4. Elliptic codes and image stability

When the observer's eye position shifts parallel to the abscissa axis from left to right and conversely, with constant interpupillary distance, the image undergoes an angular change with respect to the holo-engraving plane.

In Fig. 13 the theoretical scheme is presented, which shows the relative stability of bright points on a pair of elliptic code-curves when the observer's eyes move along the abscissa axis. Note the small vertical right-segment that joins the projections of stereoscopic points on the plane in each case. *L* and *R* are the positions of the left and right eyes, respectively. Fig. 13a shows this effect when the curves are ellipses with parameter $r > 1$, while Fig. 13b shows the effect when the curves are circumferences $(r = 1)$. Fig. 13c shows it when the curves are ellipses with $r < 1$. The shape of the encoding curve and the position of these bright points on the scratches determine the corresponding coordinates of the stereoscopic point. When the spots are on an ellipse, the image points are more or less stable, depending on the shape of the ellipse (parameter r). If the curve is a circumference a small rotation of the image-point is even appreciable. The best stability is obtained for ellipses with $a > b$, which means the parameter $r < 1$. Consequently, for elliptical encoding, an improvement of the stability of the images can be appreciated when the codification parameter r is smaller.

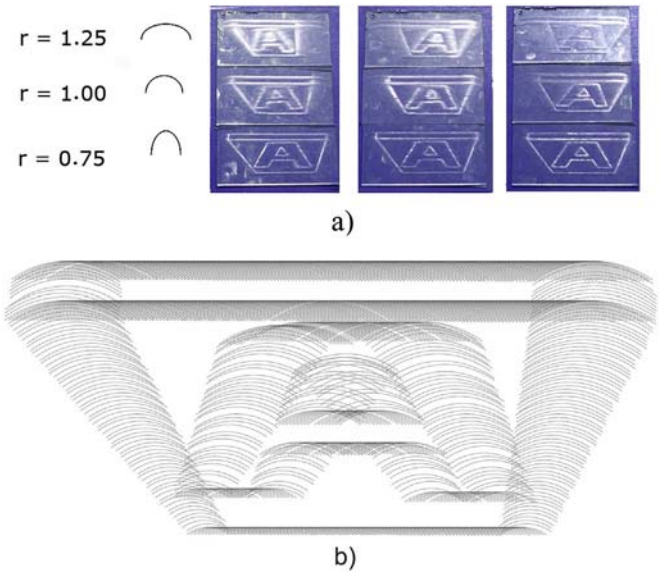

Fig. 14. Photographs of reconstructed images of a letter *A*; a) different codification parameter ***r***in elliptical codes. b) image of the computer-generated pattern corresponding to codification of the letter *A* and a polygonal reference frame by using vertical elliptic arcs with parameter $r = 0.80$.

A photographic arrangement from optically reconstructed images of a letter *A*, corresponding to the scheme above, is shown in Fig. 14. Elliptical arcs, as curvilinear codes with different r parameters, were used in the process of virtual model encoding. The columns correspond to different positions of the observer's eyes moving horizontally along the abscissa axis. An advanced version of the "3D Silhouette" software [16], allowing the elliptic encoding, was used. Each hologravure was constructed on a separated acrylic piece. Note the change in inclination observed in each column.

Note in Fig. 14a that, in correspondence with the previous results, a code with a relatively longer vertical elliptical axis produces more stable images, under lateral displacements of the observer. The best stability is observed for ellipses with parameter $r < 1$. The instability of images coded by elliptic arcs with parameter $r > 1$ can be used to produce additional effects of movement.

Other conical sections, or very general functions defined on the plane, can be used as codes with particular effects on the images.

7. Applications

As mentioned before, scratch holographic laser-engravings could be competitive in numerous fields, where diverse types of materials can be used to record the engravings. A very wide range of applications is found in Art, Graphic Design and Visual Media for Education, Information Processing, mapping and contour maps, teaching of Optics, Science, Geometry, and others, which can be broadened with the results obtained here. In [16] we can find examples of geometrical designs and the use of hologravure as a multiple information storage medium; a three-image computer-generated hologram was engraved by varying the inclination angle of the laser-traces corresponding to each object. In [18], some interesting geometric images and applications in 3D Design area are shown.

Among the applications appears the possibility of performing minimum animations. In the engravings with open circular codes, the three-dimensional images show a well-defined rotation effect around the vertical direction. Also, movement effects can be obtained by varying the form of the encoding curves, or by using slightly different curves and moving the light source or the observation point.

The use of general geometrical code shapes and our results give rise to new choices in the design of engraving-codes for specific purposes, with curves described by different symmetrical or asymmetric functions. Interesting behaviours of three-dimensional images could be obtained, giving a new and useful meaning to holographic engravings, for extending their applications and potential utility.

8. Conclusions

Based on the general principles of light ray behaviour, a geometrical theory of images was obtained. We have reported a new theoretical and experimental study on encoding image information from holograv ures, by using as codes plane curves of very general geometric shapes. This study is a contribution to a more complete background theory allowing the analysis of general curvilinear scratch-codes and their influence on 3D reconstructed images.

A variational approach of this problem allows complex cases of scratch-curves on holographic surfaces in non-homogeneous spaces to be solved. From Fermat's Principle in Optics, we proved theoretically that plane curves of general geometrical shapes can be used as curvilinear codes onto two-dimensional engravings, and the observation conditions of these images were obtained. Our model and results are applicable for other similar types of flat holographic engravings obtained on adequate materials by any non-laser method. Systems of equations allow cases of image observation to be analysed in modes of reflection and transmission of light. This point of view allows the design of engraving codes for specific purposes, making it possible to widen diverse applications. Notable effects on the images recovered optically from the engravings were observed, in agreement with theoretical results, and appropriate interpretations were considered. Image distortion was not analysed, but is the subject of future work. Particular cases of circular and elliptical codes were studied; however, a more complete and detailed theoretical study of the possibilities of the conic sections, polynomial systems, or other sets of functions, each considered as a set of particular curvilinear codes, as well as complex cases of curved surfaces, the internal profile of the grooves, the surface relief form, or the detailed analyses of possible technological processes, and its consequences, would also be of interest enough and of practical utility to be considered in forthcoming works.

Due to the reduced resolution requirements of this type of recording, and cheap support, images of relatively large size, with varied spatial effects, could be observed from greater distance, by using the appropriate illumination.

Acknowledgements

We gratefully acknowledge the collaboration and support of Laboratorio de Tecnología Láser from Instituto de Ciencia y Tecnología de los Materiales (IMRE), IMRE-Universidad de La Habana, La Habana, Cuba, for the use of the laser-engraver. Special thanks to Adalio Borges for his help with the laser-engraver system. Also, particular thanks go to Prof. Luis Berriz, from CUBASOLAR, for his help in supporting some of the materials for the engraving.

References

[1] W. Plumber, L. Gardner, Appl. Opt. 31 (1992) 6585–6588.
[2] W.J. Beaty, Hand-drawn holograms, ⟨http://www.amasci.com/amateur/holo1.html⟩.
[3] P. Kirkpatrick, Am. J. Phys. 22 (1954) 493.
[4] J.B. Lott, Math. Gaz. 47 (1963) 113–118.
[5] J. Walker, Sci. Am. 261 (1989) 106–109.
[6] N.Abramson, Hand Drawn Holography, ⟨http://hmt.com/holography/handholo.html⟩
[7] H. Weil, Improvement in advertising and like signs, UK patent 37208/34 (1934).
[8] N. Abramson, Proc. SPIE, T. Jeong and W. Sobotka Eds., 4149 (2000) 153–164.
[9]] N. Abramson, The inventor Hans Weil as a pioneer of holography, In: Holography-Jahrbuch 1989/90, Rita Witting Publishing, Germany, pp. 1–15.
[10] . Zianguirova, “Nikolai Koleitchuk”, In: Dieter Jung (Ed.), Holographic Network, Rasch Verlag Bramsche, Germany, 2003, p. 45.
[11] E. Garfield, Essays Inf. Sci. 5 (1981) 348–354.
[12] J. Eichler, L. Dünkel, O. Gonçalves, Appl. Opt. 42 (2003) 5627–5633.
[13] W. Beaty, Proc. SPIE-IS & T Electron. Imaging, SPIE 5005 (2003) pp. 156–167.
[14] M. Brand, Appl. Opt. 50 (2011) 5042–5046.
[15] T. Duke, 9th International Symposium on Display Holography (ISDH2012) IOP Publishing, Journal of Physics: Conference Series 415 (2013) 012033 doi:10.1088/1742-6596/415/1/012033.
[16] A.G. Augier, R.B. Sánchez, Opt. Commun. 284 (2011) 112–117.
[17] A.G. Augier, R.B. Sánchez, Rev. Cuba. Física 27 (2010) 107–110.
[18] A.G. Augier, R.B. Sánchez, Photonics Lett. Pol. 2 (2010) 153–155.
[19] A.G. Augier, Revista Cubana de Fisica (Special Issue-Closing the International Year of Light 2015), 33, 1E (2016) E5–E9.
[20] H.J. Caulfield, Sun Lu, The Applications of Holography, Wiley-Interscience, 1970, p. 92.
[21] A.A. Kozma, D.L. Kelly, Appl. Opt. 4 (1965) 387–392.
[22] A.W. Lohmann, D.P. Paris, Appl. Opt. 6 (1967) 1739–1748.
[23] O. Bryngdal, F. Wyrowski, Prog. Opt. 28 (1990).
[24] A.W. Lohmann, Opt. Photonics News (2008) 36–41.
[25] Holograv ure as optical printing technology ⟨http://www.science-and-design.com/holograv ure/holograv ure_definition/holograv ure_definition_01.html⟩. Or technology Geola-ilumograph-HoloCam. ⟨http://www.geola.it/it/holography_equipment/⟩.
[26] M. Minnaert, The Nature of Light & Colour in the Open Air, Dover Publications, 1954.
[27] N. Abramson, Light in Flight or the Holodiagram: The Columbi Egg of Optics, SPIE, Bellingham, Wash, 1996.